JOURNAL OF Materials CHEMISTRY

X-Ray powder diffraction and EXAFS studies on SnAPO-5 and Cu : SnAPO-5†

Wendy R. Flavell,[a] David G. Nicholson,[b] Merete H. Nilsen*[b] and Kenny Ståhl[c]

[a]*Department of Physics, UMIST, PO Box 88, Sackville Street, Manchester, UK M60 1QD*
[b]*Department of Chemistry, Norwegian University of Science and Technology, N-7491 Trondheim, Norway*
[c]*Chemistry Department, Technical University of Denmark, DK-2800 Lyngby, Denmark*

Received 3rd July 2000, Accepted 12th October 2000
First published as an Advance Article on the web 21st December 2000

SnAPO-5 was synthesised and calcined at 800 °C. Copper was introduced into the calcined material by the incipient wetness method. The as-synthesised, calcined and copper-incorporated SnAPO-5 have been studied using X-ray powder diffraction and EXAFS. Rietveld refinements show that the overall microporous $AlPO_4$-5 framework is unaffected by the incorporation of tin or copper. EXAFS shows that tin substitutes for aluminium and/or phosphorus, with an oxygen multiplicity between five and six. X-Ray powder diffraction confirms that tin substitutes into the framework on positions that are close to the tetrahedral faces. Based on crystal chemical considerations it is suggested that tin is five-coordinate in a trigonal bipyramid with its second axial corner protruding into the extra-framework area. For the copper-incorporated material, Cu : SnAPO-5, EXAFS shows that the copper environment is tetragonally distorted octahedral. Powder diffraction confirms an extra-framework disordered square-planar copper-coordination connected to two framework oxygens by longer axial bonds. EXAFS results of calcined Cu : SnAPO-5 show that copper is sited near the tin sites in the framework.

Introduction

A number of studies have been carried out on the reduction of NO_x using zeotypes as catalysts.[1–12] In the case of the zeolite ZSM-5, it has been found that conversions of NO to N_2 vary from a low of 20%[13] to a high of 100%[14] for the ion-exchanged tin(IV) and copper(II) materials, respectively.

In this paper we focus on the aluminophosphate $AlPO_4$-5,[15] a formally neutral zeotype, rather than the charged lattice of a zeolite. In the case of $AlPO_4$-5, incorporation of metal atoms occurs by processes other than ion-exchange. One of these processes is to modify the microporous framework by substituting aluminium or phosphorus by a few percent of selected metal atoms in different valence states.[16] This can lead to the lattice acquiring a charge, the magnitude of which depends on whether the valence state of the substituting metal differs from that of the framework atom being substituted.

Most substitutions are with divalent metal atoms and appear to occur at the aluminium positions.[17] However, there are indications that copper(II) substitutes at the phosphorus sites in $AlPO_4$-5.[18,19] It has also been suggested that substitution at the same sites applies to tin(IV), the resulting material being known as SnAPO-5.[20,21] Since there is a considerable size difference between tin(IV) and Al(III)/P(V) (*ca.* 0.4 Å) the framework must distort around the few sites involved in order to accommodate the larger metal atoms. In addition, the valence state of tin results in a charge being introduced to the framework. Since these changes may affect the uptake and distribution of copper(II) relative to the parent $AlPO_4$-5 we considered it of interest to compare and contrast the two materials as supports for copper(II) in the catalysts Cu : $AlPO_4$-5 and Cu : SnAPO-5, the copper being incorporated by the incipient wetness method.

†Powder XRD details are available as electronic supplementary information (ESI). See http://www.rsc.org/suppdata/jm/b0/b005321j/

X-Ray absorption spectroscopy (XANES, EXAFS) is widely used in the study of local environments of metal atoms incorporated into MeAPOs.[19,22–25] EXAFS is useful for probing the local coordination of a specific element in a sample, and can yield estimates of the number and type of atoms surrounding the central absorbing atom, together with an accurate determination of the interatomic distances. Whereas EXAFS is sensitive to the local atomic environment about a selected element, X-ray diffraction probes the overall long-range structure of the solid. EXAFS, together with Rietveld refinements[26] of powder X-ray diffraction data, is a particularly powerful combination in structural studies on zeotypes.

We report here a combined XAS (Sn and Cu K-edges) and X-ray powder diffraction study on SnAPO-5 and copper-incorporated SnAPO-5 (Cu : SnAPO-5). The results show that tin is penta-coordinated and sited in the framework. In Cu : SnAPO-5, copper is in an extra-framework disordered square-planar coordination connected to two framework oxygens by longer axial bonds. After calcination, copper moves into positions that are part of the local environment about the framework-substituted tin atoms.

Experimental

Preparation of SnAPO-5

SnAPO-5 sample was synthesised according to the method of Tapp and Cardile.[20] The composition of the synthesis gel was 1.4 TEA : 0.2 SnO_2 : 1.0 Al_2O_3 : 1.0 P_2O_5 : 40 H_2O. A slurry, prepared from pseudo-boehmite (6.03 g; AlOOH, BA Chemical Ltd.), was dissolved in distilled water (20 ml) and orthophosphoric acid (9.8 g; H_3PO_4, 85 wt.%, Merck) and stirred for one hour. To this mixture was added tin(IV) chloride pentahydrate (3.45 g; $SnCl_4 \cdot H_2O$, 98%, Aldrich) dissolved in

 DOI: 10.1039/b005321j

water (16 ml). The stirring was continued for 1.5 hours, before the template, triethylamine (7.10 g; TEA, $<0.2\%$ H_2O, Merck) was added. The pH increased to 3 on adding the template. The resulting gel was stirred for three hours, and then sealed in a Teflon-lined autoclave and kept at 90 °C for 96 hours, before heating to 200 °C at autogeneous pressure for 24 h. The white crystalline product was filtered, washed with distilled water and dried in air at room temperature. The pH of the mother liquor after crystallisation was 7. The template was removed by calcining the as-synthesised product at 800 °C for 24 h.

Copper was attached to the calcined materials using the incipient wetness method. This involved adding copper nitrate solution (1.0 M, corresponding to 1.0 g) to SnAPO-5 (1.2 g). The product was turquoise, and changed to light green upon calcination at 550 °C for 24 h.

Characterisation

The materials were analysed for copper and tin by atomic absorption spectroscopy (AAS) on a Perkin Elmer 1100 B AAS using the flame emission technique for tin determination, and a regular flame technique for copper. A scanning electron micrograph was taken on a Zeiss Scanning Electron Microscope DSM 940.

Powder X-ray diffraction measurements

The powder diffractograms were obtained using a Philips PW3710 diffractometer with copper radiation [$\lambda(K\alpha_1)=1.54056$, $\lambda(K\alpha_2)=1.54439$ Å], in the 2θ range 5–130°, for 37 s per step. The intensities were corrected for variations due to the auto-divergence slit. CCDC 1145/256. See http://www.rsc.org/suppdata/jm/b0/b005321j/ for crystallographic files in .doc format.

Rietveld refinement

The Rietveld program used in this work is a local variant of the LHMP1 program by Hill and Howard.[27] The program minimises the quantity $\Sigma_i w_i(Y_{io}-Y_{ic})^2$ with $w_i=1/Y_{io}$ and Y_{io} being the intensity before background subtraction. Pseudo-Voigt profile functions were used in all refinements with one asymmetry, one Lorentzian component and two half-width (FWHM $=V(\tan\theta+W)^{1/2}$) parameters being refined. The 2θ zero point was refined as well as one asymmetry parameter and the overall temperature factor coefficient. Scattering factors and anomalous scattering corrections were taken from *International Tables for X-Ray Crystallography.*[28]

EXAFS data collection

X-Ray absorption measurements at the Sn K-edge ($\lambda=0.4247$ Å, $E=29.195$ eV) were carried out at the wiggler beam line 9 (station 9.2) and at the Cu K-edge ($\lambda=1.38043$ Å, $E=8979$ eV) at the bending magnet beam line 7 (station 7.1) at the Synchrotron Radiation Source (SRS, 2.0 GeV, max current 200 mA), Daresbury Laboratory, UK.

At station 9.2, the monochromator is a double-crystal Si(220) single crystal. The fluorescence spectra were measured using a Canberra multielement (12) detector.[29] At station 7.1, the appropriate X-ray wavelength was selected by a Si(111) double crystal monochromator that was offset to 50% of the rocking curve for harmonic rejection. Gas ion chambers were used for measuring the intensities of the incident (I_0) and transmitted (I_t) X-rays. The first ion chamber was filled with Ar at a partial pressure of 47 Torr and the second ion chamber with Ar at a partial pressure of 338.6 Torr, both being filled to atmospheric pressure with He; these gas mixtures account for 20% and 80% absorption, respectively.

The amounts of material in the samples were calculated from element mass fractions and the absorption coefficients of the constituent elements[30] above the absorption edge to give an absorber optical thickness of 1.5 (0.1 for fluorescence mode) absorption lengths. The well-powdered (50–100 mg) samples were mixed with boron nitride so as to obtain a homogeneous sample thickness of *ca.* 1 mm for a surface area of 2 cm^2, placed in aluminium sample holders and held in place by Kapton tape windows. Several scans were collected and summed for each sample.

EXAFS data analysis

The data were corrected for dark currents, summed and background subtracted to yield the EXAFS function $\chi^{obs}_i(k)$ by means of the EXCALIB and EXBACK programs.[31] Model fitting was carried out with EXCURV90,[31] using curved-wave theory and *ab initio* phase shifts calculated within EXCURV90. The low energy cut-off for all samples was 30 eV, and a k^3 weighting scheme was used. Low-frequency contributions were removed as described previously.[24]

Tin(IV) oxide,[32] copper(II) hydroxide[33] and copper(II) oxide[34] were used as reference compounds for tin and copper, respectively, to check the validity of the *ab initio* phase shifts and to establish the general parameters, AFAC (the amplitude reduction) and VPI (the constant imaginary potential used to describe the lifetime of the photoelectron).[35] These parameters were transferred into the analyses for the unknown compounds, thereby reducing any residual systematic error in the multiplicities.

The EXAFS spectra were least squares fitted using k^1 and k^3 weighted data. Coupling between N (multiplicity) and $2\sigma^2$ (Debye–Waller-type factor) was reduced by choosing solutions common to both weighting schemes.[36]

In order to obtain meaningful results, it is essential to identify the maximum number of independent parameters, N_{ind}, that may be varied in the EXAFS analysis. This is given by $N_{ind}=2\Delta k\Delta R/\pi$ where Δk is the extent of the data in k-space and ΔR the range of distance being modelled. Another constraint is the smallest separation of shells that can be resolved. This is given by $\pi/\Delta k$.[37] For these analyses $N_{ind}=12$ and $\pi/\Delta k=0.26$ Å for data collected on the Sn K-edge. For the data collected on the Cu K-edge, $N_{ind}=6$ and 12 for the as-synthesised and calcined samples, respectively, and $\pi/\Delta k=0.29$ Å. The addition of successive shells was tested for significance using the procedure of Joyner *et al.*[38]

Results and discussion

Characterisation

The X-ray diffractograms of as-synthesised, calcined and copper-incorporated SnAPO-5 (Fig. 1) confirm that the materials have the $AlPO_4$-5 (AFI) structure,[15] hence, they are thermally stable up to 800 °C and this stability is little affected by the incorporation of copper. The AAS analysis on SnAPO-5 yields a tin content of 4.0% and shows that the sample incorporating copper contained 2.3% of that metal. Scanning electron microscopy of the calcined SnAPO-5 material (Fig. 2) reveals hexagonal particles which are fairly regular in shape and approximately 20–25 μm in length.

The overall framework

Rietveld refinements establish that tin substitutes into the aluminophosphate framework without affecting the overall microporous structure. The diffraction patterns and final fits for the samples are shown in Fig. 1. The parameters from the Rietveld refinements are listed in Table 1, the refined coordinates are given in Table 2 and some selected distances are presented in Table 3.

The refinements started with parameters for the pure $AlPO_4$-5 framework.[39] Since the space group (*P6/mcc*) does not differ-

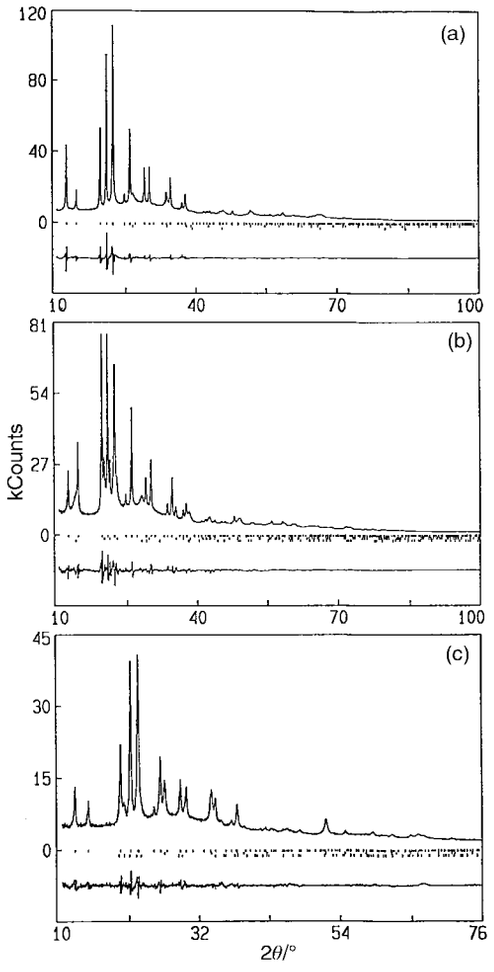

Fig. 1 Diffraction patterns and final difference patterns for SnAPO-5 materials: (a) as-synthesised; (b) calcined; (c) copper incorporated.

entiate between aluminium and phosphorus, the framework atoms are denoted as T-atoms. The four T–O distances (average 1.62 Å) and the four Al···P (average 3.10 Å) are consistent with those reported for $AlPO_4$-5.[39] The frameworks of as-synthesised, calcined and copper-incorporated SnAPO-5 are similar, while the extra phases found in the calcined SnAPO-5 differ from those detected for the as-synthesised and copper-incorporated samples (Table 1).

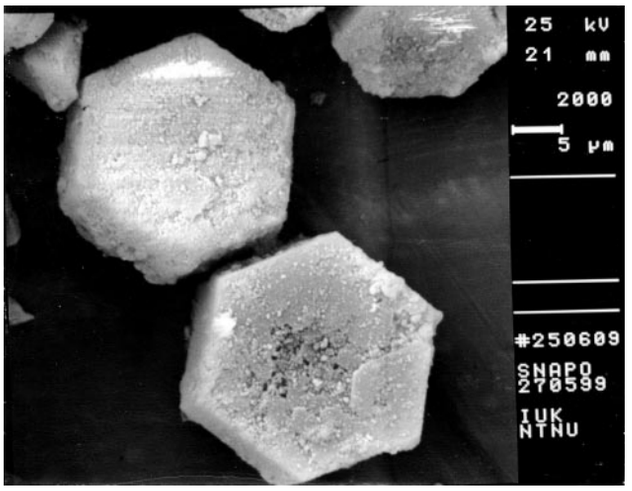

Fig. 2 Scanning electron micrograph of calcined SnAPO-5.

Tin environment in SnAPO-5

The local environment of tin in the SnAPO-5 materials was first studied by EXAFS since this information helps in defining the model to be refined against the diffraction data. The results from the Sn K-edge are shown in Table 4, and the spectra and their Fourier transforms in Fig. 3.

The second shell in the Fourier transformed EXAFS is a valuable indicator for framework substitution, because metals substituted into some of the T sites of the zeotype lattice generally lead to four Me···T distances of *ca.* 3.1 Å.[40] The atomic numbers for the T-atoms (Al and P) are too similar for EXAFS to unequivocally distinguish between the groupings $Sn\cdots(Al)_4$ and $Sn\cdots(P)_4$. Since tin has been shown to substitute for phosphorus,[20,21] aluminium was chosen to represent both T-atoms. The feature at 3–4 Å in the Fourier transformed EXAFS fitted well to four Sn···Al distances at 3.3 and 3.8 Å.

For aluminophosphates with a metal (M) tetrahedrally substituted into the framework the multiplicity of the M–O distance is four. For SnAPO-5, the distances of the first shell (Sn–O) (multiplicities of five–six and distances at 2.03 Å) are significantly longer than in a tetrahedral environment (1.95 Å[41]). The EXAFS shows, in agreement with the XRD results (Table 1) that SnO_2 is not present to a significant degree. This is shown by comparing the experimental EXAFS of SnO_2 (Fig. 4) with the EXAFS of SnAPO-5 (Fig. 3).

From the EXAFS of the three tin-containing materials it is evident that tin is sited in the framework in a non-tetrahedral coordination position.

Table 1 Refinement data for SnAPO-5 materials. Space group *P6/mcc*

	As-synthesised	Calcined	Cu-incorporated
R_p (%)[a]	3.98	3.91	3.34
R_{wp} (%)[b]	4.89	4.70	4.18
GOF[c]	3.99	3.55	2.33
R_B (%)[d,f]	0.96	1.15	0.55
No. of parameters	47	55	44
No. of observations	4451	4451	3401
No. of Bragg reflections[f]	520	523	309
Range of 2θ/°	10–100	10–100	10–79
No. of background parameters[e]	14	15	11
Refined phases (quantity[g] in %)	SnAPO-5 (87) SnO_2 (0.1) γ-Al_2O_3 (12.9)	SnAPO-5 (70) AlPO-tridymite (21) boehmite (9)	SnAPO-5 (93.5) SnO_2 (0.2) AlPO-tridymite (6.3)
a/Å	13.6965(12)	13.6935(14)	13.7579(24)
c/Å	8.4231(4)	8.4689(5)	8.3604(8)
Volume/Å^3	1368	1375	1370

[a] $R_p = \sum |Y_{io} - Y_i| / \sum Y_{io}$. [b] $R_{wp} = (\sum w_i(Y_{io} - Y_i)^2 / \sum w_i(Y_{io})^2)^{1/2}$. [c] $GOF = \sum w_i(Y_{io} - Y_i)^2/(n-p)$. [d] $R_B = \sum |I_{ko} - I_k| / \sum I_{ko}$. [e] Chebyshev type I. [f] These values refer to the SnAPO-5-phases. [g] These values are calculated according to ref. 48.

Table 2 Refined fractional coordinates ($\times 10^4$), temperature-factor coefficients and occupancy factors (g) for SnAPO-5 materials[a]

	x	y	z	B/Å^2	g
As-synthesised SnAPO-5					
Al	4542(5)	3306(4)	1855(5)	1.2	0.508(4)
P	4542(5)	3306(4)	1855(5)	1.2	0.508(4)
O(1)	4169(9)	2084(5)	2500	2.0	0.500
O(2)	4732(12)	3643(11)	0	2.0	0.500
O(3)	3560(11)	3560(11)	2500	2.0	0.500
O(4)	5818(6)	4183(6)	2500	2.0	0.500
Sn(2)	4986	1598	1301	1.2	0.033(1)
Sn(3)	3523	2278	881	1.2	0.021(1)
O(A)	6667	3333	0	3.0	0.036(3)
O(B)	1864	1563	0	3.0	0.186(7)
O(C)	1850	468	1415	3.0	0.188(14)
Calcined SnAPO-5					
Al	4568(4)	3352(4)	1809(5)	1.2	0.453(4)
P	4568(4)	3352(4)	1809(5)	1.2	0.453(4)
O(1)	4163(7)	2082(3)	2500	2.0	0.500
O(2)	4465(10)	3148(10)	0	2.0	0.500
O(3)	3578(9)	3578(9)	2500	2.0	0.500
O(4)	5769(4)	4231(4)	2500	2.0	0.500
O(5)	4520	3373	5000	3.0	0.145(4)
Sn(1)	4569	3373	2700	1.2	0.064(2)
O(A)	1279	540(27)	1170(18)	3.0	0.400(10)
O(B)	0	0	2500	3.0	0.037(3)
O(C)	2579	665	0	3.0	0.068(7)
O(D)	1878	1464	0	3.0	0.097(9)
Copper incorporated SnAPO-5					
Al	4621(5)	3315(6)	1845(7)	1.2	0.462(5)
P	4621(5)	3315(6)	1845(7)	1.2	0.462(5)
O(1)	4107(12)	2053(6)	2500	2.0	0.500
O(2)	4783(16)	3665(15)	0	2.0	0.500
O(3)	3502(13)	3502(13)	2500	2.0	0.500
O(4)	5775(7)	4225(7)	2500	2.0	0.500
Sn(2)	4986	1598	1301	1.2	0.022(1)
Sn(3)	3523	2278	881	1.2	0.017
O(A)	6667	3333	0	3.0	0.039
O(B)	1465	1234	0	3.0	0.066
O(C)	1850	468	1415	3.0	0.178
O(D)	358	1688	2608	3.0	0.099

[a]Numbers in the parentheses are the e.s.d.s in the units of the least significant digit given. Parameters without e.s.d.s were held fixed in refinement.

The framework siting of tin is confirmed by the Rietveld refinement, with the difference Fourier map showing significant residual electron density near the framework atoms (Al and P) which decreased on placing 4% tin at this position. Since tin is sited near the framework sites, the position could not be refined (tin being initially placed on a phosphorus position), but the coordinates were adjusted to minimise the difference density and to improve the fit. Further examination of the difference map showed that tin is penta-coordinated to four framework oxygens and one extra-framework oxygen thereby completing a trigonal bipyramid. Such a bipyramidal arrangement does not significantly disturb the overall framework structure

Table 3 Selected distances (Å) from the Rietveld refinements

As-synthesised sample		Calcined sample		Copper-incorporated sample	
Al/P–O(1)	1.581(9)	Al/P–O(1)	1.647(6)	Al/P–O(1)	1.608(10)
–O(2)	1.613(5)	–O(2)	1.551(5)	–O(2)	1.598(8)
–O(3)	1.642(7)	–O(3)	1.642(6)	–O(3)	1.770(9)
–O(4)	1.641(9)	–O(4)	1.587(7)	–O(4)	1.549(10)
Mean	1.619	Mean	1.608	Mean	1.631
Al–P	3.036(7)	Al–P	3.063(6)	Al–P	2.973(10)
	3.124(6)		3.080(10)		3.043(10)
	3.128(7)		3.112(7)		3.085(8)
	3.142(7)		3.151(10)		3.300(10)
Mean	3.108	Mean	3.102	Mean	3.100

Table 4 Results of EXAFS curve-fitting (k-range 3–15 Å^{-1}) on the Sn K-edge.[a] A: as-synthesised SnAPO-5; B: calcined SnAPO-5; C: as-synthesised Cu : SnAPO-5

Sample		N[b]	r/Å	$2\sigma^2$/Å^2	E_0/eV	R (%)
A	Sn–O	6.0	2.031(2)	0.011(1)	16.2(3)	29.2
	Sn···Al[c]	2.0	3.28(1)	0.013(3)		
	Sn···Al[c]	2.0	3.58(1)	0.013(3)		
B	Sn–O	5.5	2.033(1)	0.012(1)	15.0(2)	24.6
	Sn···Al[c]	2.0	3.26(1)	0.016(3)		
	Sn···Al[c]	2.0	3.54(2)	0.019(4)		
	Sn···Sn	1.0	3.681(6)	0.011(1)		
C	Sn–O	6.0	2.027(2)	0.010(1)	16.1(3)	29.9
	Sn···Al[c]	2.0	3.31(1)	0.012(3)		
	Sn···Al[c]	2.0	3.59(2)	0.014(4)		

[a]Each bonding distance (R) is associated with a coordination number (N) and thermal vibration and static disorder (Debye–Waller-like factor, $2\sigma^2$). E_0 is the refined correction to the threshold energy of the absorption edge. The spectra were Fourier filtered using a Gaussian window function, 1.0–25.0 Å. The standard deviation in the least significant digit as calculated by EXCURV90 is given in parentheses. However, note that such estimates of precision overestimate the accuracy, particularly in cases of high correlation between parameters. The estimated standard deviations for the distances are 0.01 Å at $R<2.5$ Å, with $\pm 20\%$ accuracy for N and $2\sigma^2$, although the accuracy for these is increased by refinements using k^1 *vs.* k^3 weighting (see main text). Residual index R was calculated as

$$R = \frac{\sum_i [(\chi_i^{\mathrm{exp}} - \chi_i^{\mathrm{calc}})k^{WT}]^2}{\sum_i [(\chi_i^{\mathrm{exp}})k^{WT}]^2}$$

[b]Except for the first shell for B, the multiplicities were fixed in the final refinements at the integer closest to the values returned by the full refinements. [c]See text.

because the additional (fifth) coordination perturbs the extra-framework area. Projections of the structures are shown in Fig. 5. From the EXAFS (Table 4) the tin is coordinated to five–six oxygens, the lower figure being consistent with the Rietveld analysis.

The results show that substitution of *ca.* 4% tin into an originally tetrahedral network leads to significant local structure changes of the framework through an increase in coordination. It is known that zeotype frameworks are amenable to small degrees of substitution; thus, the reluctance of some metals to be tetrahedrally coordinated by oxygen (*e.g.* titanium in titanium silicalite-1[42] and copper in CuAPO-5[19]) is manifested through five- and six-coordination. Although a tetrahedral framework siting is consistent with the general chemistry of tin, an expansion of the coordination number can be rationalised in terms of the large size of tin(IV).

In metal-substituted aluminophosphates, the metals are uniformly distributed over the framework. Since the metal contents are low in these materials, local M···M distances cannot be present in samples with high distribution.[43] However, the EXAFS of calcined SnAPO-5 does exhibit a Sn···Sn distance at 3.68 Å. This result is in agreement with the results of Rietveld refinements, which show that the structure adjusts itself upon calcination in a manner that ensures that tin substitution occurs in pairs connected by a bridging oxygen, as depicted in Fig. 5. The migration of tin atoms to form Sn–Sn pairs does not induce an overall change in structure because the number of tin atoms is small and the $AlPO_4$-5 lattice is flexible enough to adjust to local changes.

The copper environment in Cu : SnAPO-5

The XANES (with their first derivatives) of as-synthesised and calcined Cu : SnAPO-5 are shown in Fig. 6, together with those for model compounds copper(II) oxide and copper(II) hydr-

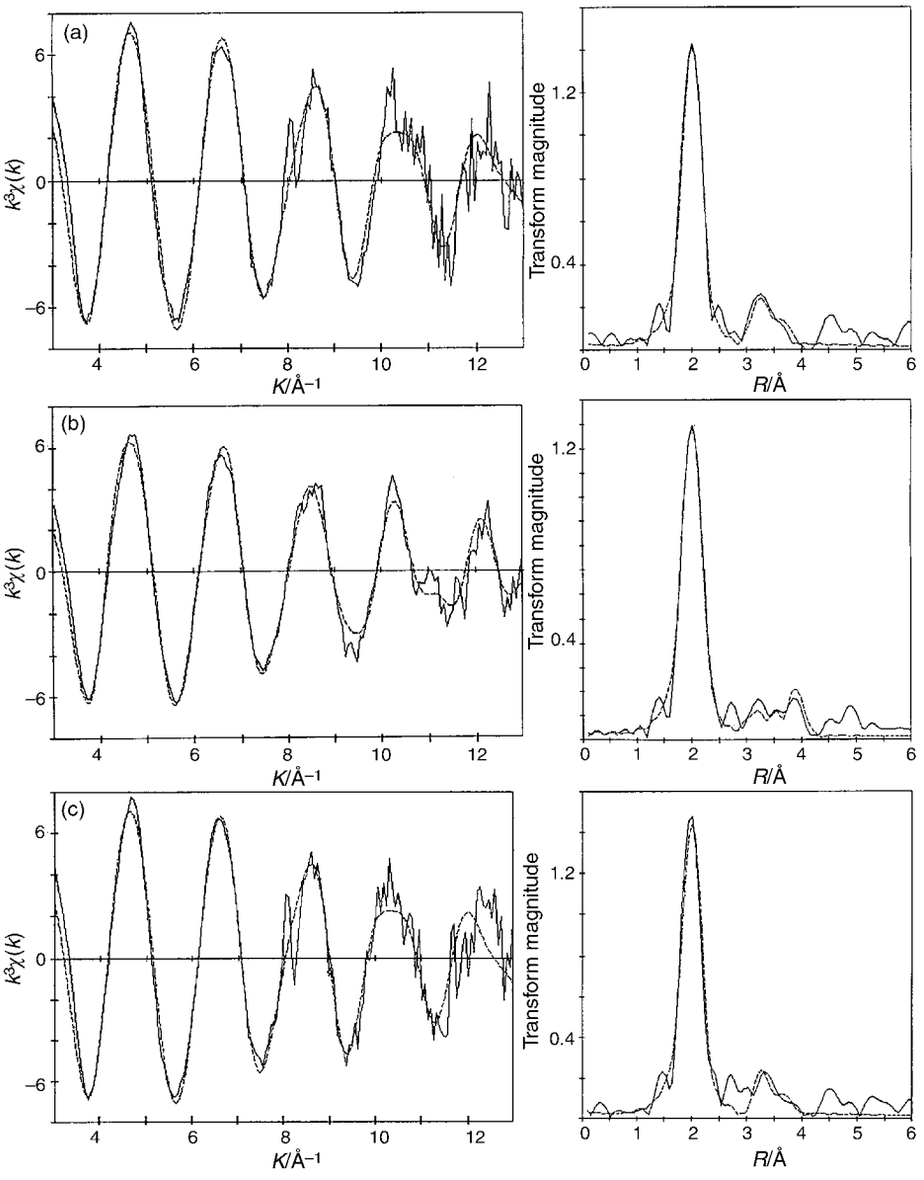

Fig. 3 Experimental (—) and calculated (---) Fourier filtered (1.0–25.0 Å) k^3-weighted EXAFS and their Fourier transforms for SnAPO-5 materials, Sn K-edge: (a) as-synthesised; (b) calcined; (c) copper incorporated.

oxide. The XANES of copper(II) oxide has a characteristic shoulder at 8991 eV which is attributed to the 1s⟶4p transition with accompanying ligand-to-metal charge transfer and shake-down transitions.[44–46] The first derivatives of the edge regions (Fig. 6) are also shown because they are useful for establishing transition energies and, in particular, highlighting characteristic features.[24] This is nicely illustrated by the derivative spectra of copper(II) oxide and calcined Cu : SnAPO-5 which show large differences and hence are consistent with the absence of copper(II) oxide in the latter material. It is also clear from the XANES (particularly the first derivative spectra) of the present materials that autoreduction does not occur (ref. 19 and references therein).

The EXAFS analyses of the as-synthesised and calcined

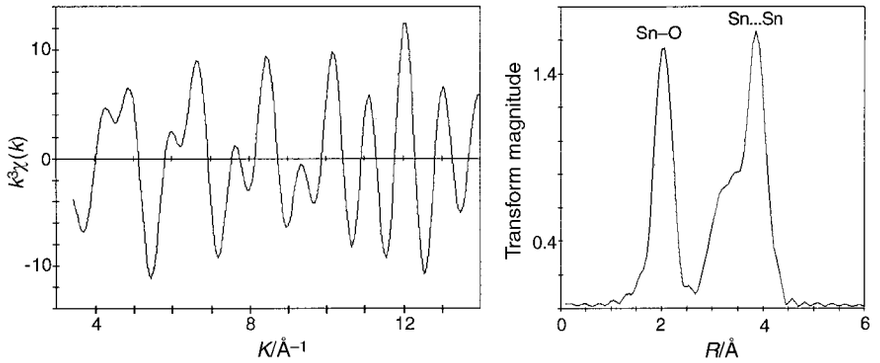

Fig. 4 Experimental (—) Fourier filtered (1.0–25.0 Å) k^3-weighted Sn K-edge EXAFS and the Fourier transform for SnO_2.

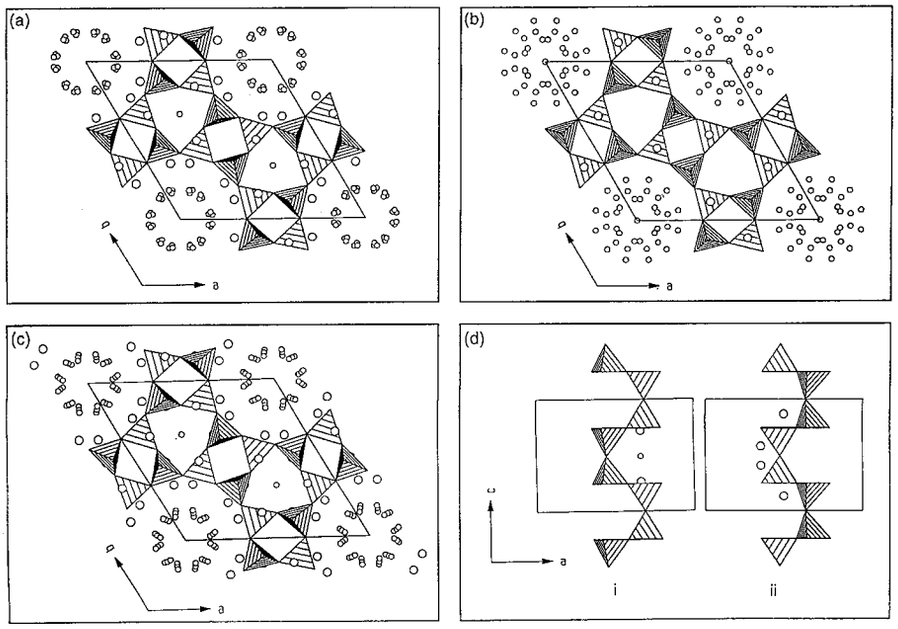

Fig. 5 The *ab*-projections of (a) as-synthesised SnAPO-5; (b) calcined SnAPO-5 and (c) as-synthesised Cu : SnAPO-5. The circles show the statistical positions refined as tin (large circles) and oxygen (small circles). The *ac*-projection (d) shows the bridging oxygen between two framework-substituted tin atoms for calcined SnAPO-5 (ii), which is not seen in the as-synthesised SnAPO-5 (i).

Cu : SnAPO-5 materials are given in Table 5 and the spectra and their Fourier transforms are shown in Fig. 7. For as-synthesised Cu : SnAPO-5, the EXAFS results together with the turquoise colour of the material show that the copper environment is essentially tetragonally distorted octahedral. As previously reported,[19,46] the long axial Cu–O distances in similar copper environments are not readily apparent in the EXAFS Fourier transforms. This has been attributed to a combination of large Debye–Waller-type factors and interference with oscillations from more distant shells. However, in Cu : SnAPO-5 the axial bonds appear in the Fourier transforms, which is consistent with the relatively low Debye–Waller factors ($2\sigma^2$) for this shell (0.011 Å^2).

In the Rietveld refinement of as-synthesised Cu : SnAPO-5, the extra-framework positions were located from difference Fourier maps. The interpretation of these sites was based on the EXAFS model. The atom O(C) in Cu : SnAPO-5 (Table 2) was shown to represent the copper. Non-framework oxygens at an average distance of *ca.* 2.0 Å form a square plane, and two framework oxygens (at 2.8–2.9 Å) complete the distorted octahedral coordination.

The EXAFS results of calcined Cu : SnAPO-5 show that copper again is in a tetragonally distorted octahedral environment with the axial oxygens being linked to the framework, consistent with EXAFS and Rietveld results of the as-synthesised sample.

A comparison of the EXAFS results for Cu : SnAPO-5 with the EXAFS reported[47] for as-synthesised and calcined Cu:$AlPO_4$-5 shows that the substitution of tin creates sites that are more amenable to copper than to aluminium/phosphorus. The AAS-analyses show that Cu : SnAPO-5 contains less copper than Cu : $AlPO_4$-5 (2.3 and 5.7%, respectively), indicating that the presence of tin prevents uptake of larger amounts of copper. This may be caused by tin blocking the pores, as suggested by Tapp and Cardile.[20]

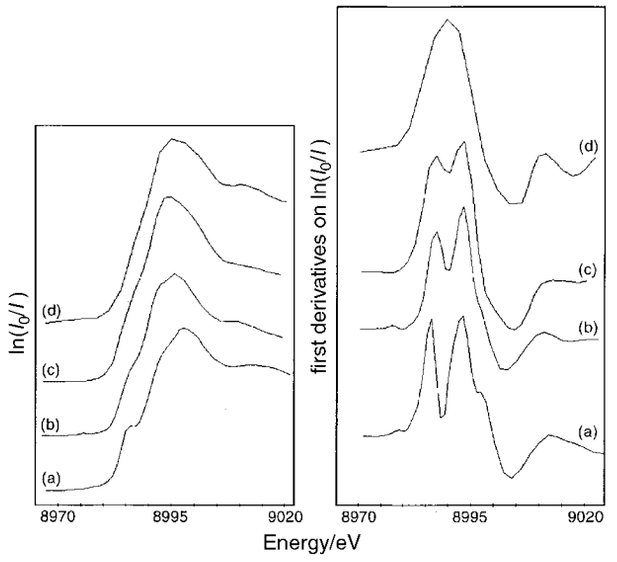

Fig. 6 Normalised Cu K-edge XANES and the first derivatives of (a) copper(II) oxide; (b) copper(II) hydroxide; (c) as-synthesised Cu : SnAPO-5; (d) calcined Cu : SnAPO-5.

Conclusions

(i) Rietveld refinements of SnAPO-5 and Cu : SnAPO-5 show that the overall microporous framework is little affected by

Table 5 Results of EXAFS curve-fitting (k-range 3–14 Å^{-1}) on the Cu K-edge.[a] A: as-synthesised Cu : SnAPO-5; B: calcined Cu : SnAPO-5

Sample		N^b	r/Å	$2\sigma^2$/Å^2	E_0/eV	R (%)
A	Cu–O	4.0	1.922(1)	0.009(1)	26.8(3)	22.4
	Cu–O	2.0	2.66(2)	0.029(6)		
B	Cu–O	4.0	1.887(3)	0.014(1)	26.7(3)	35.9[c]
	Cu–O	2.0	2.606(2)	0.022(5)		
	Cu···Cu	2.0	2.893(5)	0.016(1)		
	Cu···Sn	1.0	3.164(5)	0.010(1)		

[a]See footnote *a* of Table 4. [b]See footnote *b* of Table 4. [c]The fit is good for backscatterers up to 4 Å from the central atom (the *R*-factor is 20.7 for the Fourier filtered (0–4 Å) spectrum), but there are also significant contributions from backscatterers further out (4–6 Å) which are attributed to distant tin atoms. Since these are not included in the fit the overall *R*-factor is higher.

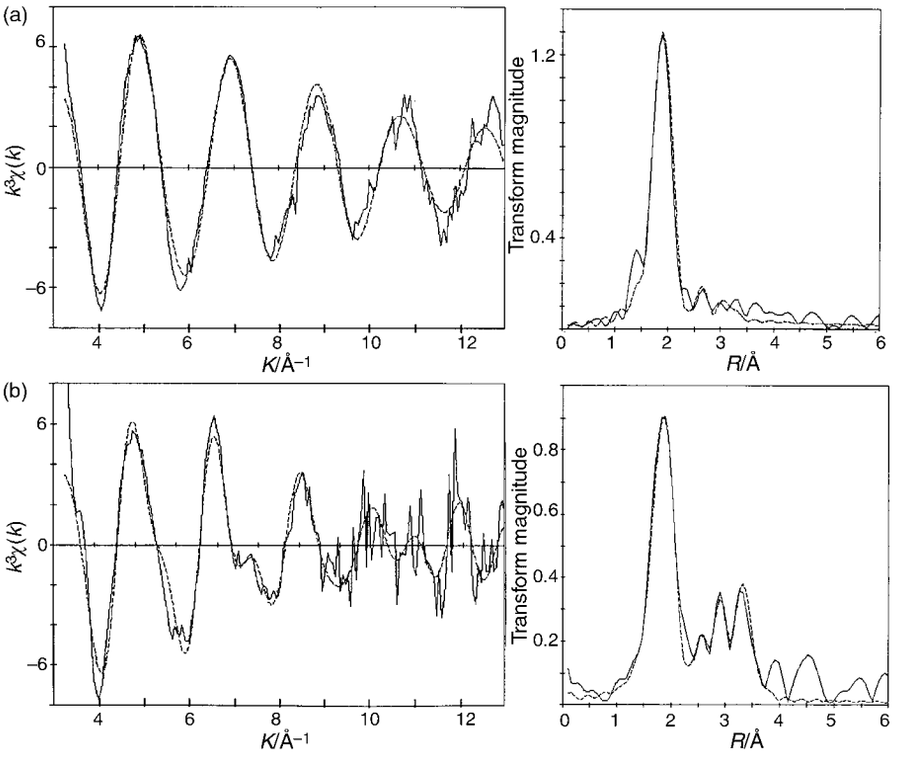

Fig. 7 Experimental (—) and calculated (---) Fourier filtered (1.0–25.0 Å) k^3-weighted EXAFS and their Fourier transforms for Cu-incorporated SnAPO-5 material, Cu K-edge: (a) as-synthesised; (b) calcined.

framework substitution by tin or by incorporating copper. (ii) EXAFS shows that tin is substituted into the framework with a multiplicity between five and six. The substitution is confirmed by the presence of four T-atoms at 3.3–3.6 Å. Rietveld refinements show residual electron density near the framework T-sites in accordance with 4% tin substitution. The combined EXAFS and Rietveld analyses are consistent with five-coordinate tin in a trigonal bipyramid, where oxygen atoms constituting the tetrahedral framework occupy four of the positions with the fifth (axial) site protruding into the extra-framework area. (iii) In as-synthesised Cu : SnAPO-5, copper is six-coordinated in a tetragonally distorted $Cu(O)_6$ octahedron, consistent with its turquoise colour and the EXAFS analysis. This stereochemistry is confirmed by the Rietveld refinements. The Rietveld refinements show that copper is attached to the framework through the two axial bonds of the distorted octahedron. This is consistent with the relatively low Debye–Waller factors in the EXAFS analysis. (iv) On calcining Cu : SnAPO-5 at 550 °C, copper moves into positions that are part of the local environment about the framework-substituted tin atoms.

Acknowledgement

Grants from the Nordic Academy of Advanced study (NorFA) and the Nansen Foundation are gratefully acknowledged (M. H. N.). The assistance of Drs. Kan-Cheung Cheung and Gert van Dorssen at stations 7.1 and 9.2 (SRS), respectively, is much appreciated. We are also very grateful to Drs. Robert Hoyle and Dr. Md. Moinuddin Sarker for help with the data collection.

References

1 M. Iwamoto and H. Hamada, *Catal. Today*, 1991, **10**, 57.
2 M. Iwamoto, H. Yahiro, K. Tanda, N. Mizuno, Y. Mine and S. Kagawa, *J. Phys. Chem.*, 1991, **95**, 3727.
3 Y. Kuroda, R. Kumashiro, T. Yoshimoto and M. Nagao, *Phys. Chem. Chem. Phys.*, 1999, **1**, 649.
4 W. Grünert, N. W. Hayes, R. W. Joyner, E. S. Shpiro, M. R. H. Siddiqui and G. N. Baeva, *J. Phys. Chem.*, 1994, **98**, 10832.
5 T. Ishihara, M. Kagwa, F. Hadama and Y. Takita, *Stud. Surf. Sci. Catal.*, 1994, **84**, 1493.
6 G. Centi and S. Perathoner, *Appl. Catal. A: Gen.*, 1995, **132**, 179.
7 T. Inui, S. Iwamoto, K. Matsuba, Y. Tanaka and T. Yoshida, *Catal. Today*, 1995, **26**, 23.
8 M. Shelef, *Chem. Rev.*, 1995, **95**, 209.
9 G. Sankar, J. M. Thomas, G. N. Greaves and A. J. Dent, *J. Phys. IV France*, 1997, **7**, C2-871.
10 J. Dedecek, J. Cejka and B. Wichterlová, *Appl. Catal. B: Environ.*, 1998, **15**, 233.
11 M. Wark, A. Brückner, T. Liese and W. Grünert, *J. Catal.*, 1998, **175**, 48.
12 D.-J. Liu and H. J. Robota, *J. Phys. Chem. B*, 1999, **103**, 2755.
13 Y. Hirao, C. Yokoyama and M. Misono, *Chem. Commun.*, 1996, 597.
14 G. Centi, C. Nigro, S. Perathoner and G. Stella, *Catal. Today*, 1993, **17**, 159.
15 J. M. Bennett, J. P. Cohen, E. M. Flanigen, J. J. Pluth and J. V. Smith, *Am. Chem. Soc. Symp. Ser.*, 1983, **218**, 109.
16 S. T. Wilson and E. M. Flanigen, *J. Am. Chem. Soc.*, 1989, **398**, 329.
17 R. Szostak, *Molecular Sieves: Principles of Synthesis and Identification*, Van Nostrand Reinhold, 1989, p. 272.
18 T. Muñoz Jr., A. M. Prakash, L. Kevan and K. J. Balkus Jr., *J. Phys. Chem. B*, 1998, **102**, 1379.
19 D. G. Nicholson and M. H. Nilsen, *J. Mater. Chem.*, 2000, **10**, 1965.
20 N. J. Tapp and C. M. Cardile, *Zeolites*, 1990, **10**, 680.
21 K. Vinje and K. P. Lillerud, *Stud. Surf. Sci. Catal.*, 1994, **84**, 227.
22 D. W. Lewis, C. R. A. Catlow, G. Sankar and S. W. Carr, *J. Phys. Chem.*, 1995, **99**, 2377.
23 P. A. Barrett, G. Sankar, C. R. A. Catlow and J. M. Thomas, *J. Phys. Chem.*, 1996, **100**, 8977.
24 A. Moen, D. G. Nicholson. M. Rønning, G. M. Lamble, J.-F. Lee and H. Emerich, *J. Chem. Soc., Faraday Trans.*, 1997, **93**(22), 4071.
25 S. Thomson, V. Luca and R. Howe, *Phys. Chem. Chem. Phys.*, 1999, **1**, 615.

26 R. A. Young (Ed.), *The Rietveld method*, International Union of Crystallography, Oxford Science Publications, 1995.
27 R. J. Hill and C. J. Howard, Australian Atomic Energy Commision (now ANSTO) Report M112, Lucas Heights Research Laboratories, New South Wales, Australia, 1986.
28 *International Tables for X-Ray Crystallography*, ed. J. A. Ibers and W. C. Hamilton, The International Union of Crystallography, The Kynoch Press, Birmingham, UK, 1974.
29 C. Morell, R. L. Bilsborrow and G. E. Derbyshire, *Instructions to EXAFS Experiments for Using the 13-Element Germanium Detector Array*, SERC Daresbury Laboratory, Warrington, Cheshire, UK WA4 4AD.
30 *International Tables for X-Ray Crystallography*, The Kynoch Press, Birmingham, UK, 1962, vol. 3, p. 175.
31 N. Binsted, J. W. Campbell, S. J. Gurman and P. C. Stephenson, SERC Daresbury Laboratory, EXCALIB, EXBACK and EXCURV90 programs, 1990.
32 W. H. Baur and A. A. Khan, *Acta Crystallogr., Sect. B*, 1971, **27**, 2133.
33 H. Jaggi Von and H. R. Oswals, *Acta Crystallogr.*, 1961, **14**, 1041.
34 S. Åsbrink and L.-J. Norrby, *Acta Crystallogr., Sect. B*, 1970, **26**, 8.
35 S. J. Gurman, N. Binsted and I. Ross, *J. Phys. C*, 1984, **17**, 143.
36 F. W. H. Kampers, C. W. R. Engelen, J. H. C. van Hooff and D. C. Koningsberger, *J. Phys. Chem.*, 1990, **94**, 8574.
37 *Report on the International Workshops on Standards and Criteria in XAFS in X-ray Absorption Fine Structure*, ed. S. S. Hasnain, Ellis Horwood, Chichester, 1991, p. 751.
38 R. W. Joyner, K. J. Martin and P. Meehan, *J. Phys. C: Solid State Phys.*, 1987, **20**, 4005.
39 J. W. Richardson, J. J. Pluth and J. V. Smith, *Acta Crystallogr., Sect. C*, 1987, **43**, 1469.
40 A. R. Heinrich and Ch. Baerlocher, *Acta Crystallogr., Sect. C*, 1991, **47**, 237.
41 R. Marchand, Y. Pifford and M. Tournoux, *Acta Crystallogr., Sect. B*, 1975, **31**, 511.
42 P. Beherens, J. Felsche, S. Vetter, G. Schulz-Ekloff, N. I. Jaeger and W. Niemann, *J. Chem. Soc., Chem. Commun.*, 1991, 678.
43 R. Szostak, *Molecular Sieves: Principles of Synthesis and Identification*, Van Nostrand Reinhold, 1989, p. 275.
44 E. Y. Choi, I.-S. Nam, Y. G. Kim, J. S. Chung, J. S. Lee and M. Nomura, *J. Mol. Catal.*, 1991, **69**, 247.
45 S. E. Shadle, J. E. Penner-Hahn, H. J. Schugar, B. Hedman, K. O. Hodgson and E. I. Solomon, *J. Am. Chem. Soc.*, 1993, **115**, 767.
46 I. J. Pickering and G. N. George, *Inorg. Chem.*, 1995, **34**, 3142.
47 M. H. Nilsen, Ph.D. thesis, Norwegian University of Science and Technology, Department of Chemistry, 2000, to be submitted.
48 R. J. Hill and C. J. Howard, *J. Appl. Crystallogr.*, 1987, **20**, 467.